Tip-enhanced near-field Raman analysis of tip-pressurized adenine molecule

Hiroyuki Watanabe,[1,2] Yasuhito Ishida,[1] Norihiko Hayazawa,[1,3] Yasushi Inouye,[3,4,5,6,*] and Satoshi Kawata[1,3,5,6]
[1]*Department of Applied Physics, Osaka University, Osaka 565-0871, Japan*
[2]*Ashigara Research Laboratories, Fuji Photo Film Co., Ltd., Kanagawa 250-0193, Japan*
[3]*CREST, Japan Corporation of Science and Technology, Saitama 332-0012, Japan*
[4]*Graduate School of Frontier Biosciences, Osaka University, Osaka 565-0871, Japan*
[5]*Handai FRC, Osaka University, Osaka 565-0871, Japan*
[6]*RIKEN, Saitama 351-0198, Japan*
(Received 19 May 2003; revised manuscript received 5 February 2004; published 15 April 2004)

We report on near-field Raman spectra of a single nanocrystal of DNA-base adenine molecules using a silver-layer-coated apertureless probe tip of an atomic force microscope. The tip-enhanced near-field Raman spectrum shows eight Raman bands that are assigned to the normal modes of adenine molecules based on the density-functional theory (DFT) calculations. The vibrational frequencies of several bands are observed to have unambiguously shifted to the values of the corresponding bands, observed using the conventional surface-enhanced Raman-scattering spectrum of adenine molecules adsorbed on colloidal silver particles. The DFT vibrational calculations of adenine complexes involving a silver atom suggest that the Raman band shifts occur due to the deformation of adenine molecules by the silver atoms coated in the probe tip.

DOI: 10.1103/PhysRevB.69.155418 PACS number(s): 68.37.Uv, 33.20.Fb, 73.20.Mf, 42.62.Be

I. INTRODUCTION

Near-field scanning optical microscopes (NSOM) have been employed for optical imaging of nanoscale molecular distributions smaller than the diffraction limit of the light.[1–5] In particular, near-field Raman spectroscopy[6–9] facilitates nanoscale detection of molecular vibrations and chemical nanoimaging. Several groups[10–12] utilize surface-enhanced Raman scattering (SERS) to overcome such a low scattering cross section. In these studies, sample molecules were located on silver-islands film. Raman scattering from the whole molecules adsorbed on the film was amplified due to local surface plasmon polaritons, then detected with a near-field aperture probe.[10,11] With a photon scanning tunneling microscope, Ferrell and co-workers[12] also pioneeringly detected the SERS signals with sharpened fiber tip. Other groups[13–18] employed tip-enhanced Raman scattering for the amplification of Raman scattering. Wessel[19] predicted field enhancement by a small metallic particle near the samples. Since a metallic tip launches local surface plasmon polaritons[20–24] at its apex, Raman scattering of molecules located just under the metallic tip was enhanced to the extent of the detection level by the local surface plasmon polaritons. Hence the samples were illuminated with near-field light and the Raman scattering from the samples was collected with an objective in the far field. In this scheme, a substrate coated with a silver-islands film is also available for the realization of much larger amplifications.

We demonstrated the detection of the near-field Raman scattering and the Raman spectral shift imaging of organic molecules[25–27] using a metallic apertureless tip.[20,28–32] Furthermore, we reported that the near-field Raman spectra involving anomalous enhancement and large frequency shifts of the Raman bands are obtained for polycrystalline Rhodamine6G dyes employing the tip-enhanced Raman NSOM.[25] These spectral changes were interpreted to occur as a result of chemical interactions between the dye and the metallic tip.[32]

In this paper we report on the tip-enhanced near-field Raman spectroscopy of a single nano crystal of adenine (Fig. 1), a DNA base. The spectra exhibit different vibrational frequency shifts to the normal Raman spectrum of adenine crystals, and slightly different shifts to the conventional SERS spectra of adenine. In a SERS measurement, adenine has been reported to adsorb on silver substrates due to interaction through the N_1 nitrogen,[33] the N_7 nitrogen,[34–36] or the external amino group[34,35] in either a side-on[34,35] or a flat-on[37,38] orientation. Most of these discrepancies are based on the difference in calculation levels[39–47] that is the base of the assignment of the Raman spectra. According to a recent study using high-level quantum chemical calculations of an adenine molecule,[34] the interaction with silver surfaces was estimated mainly to take place under N_7 nitrogen and/or the external amino group in the side-on orientation. These substantial frequency shifts could be caused by an interaction between the adenine molecule and the metal surface. The interaction is well known as a cause of the charge transfer

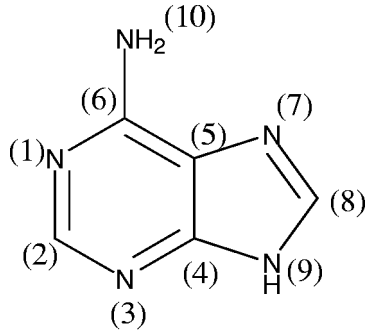

Adenine

FIG. 1. Molecular structure and atomic numbering of adenine.

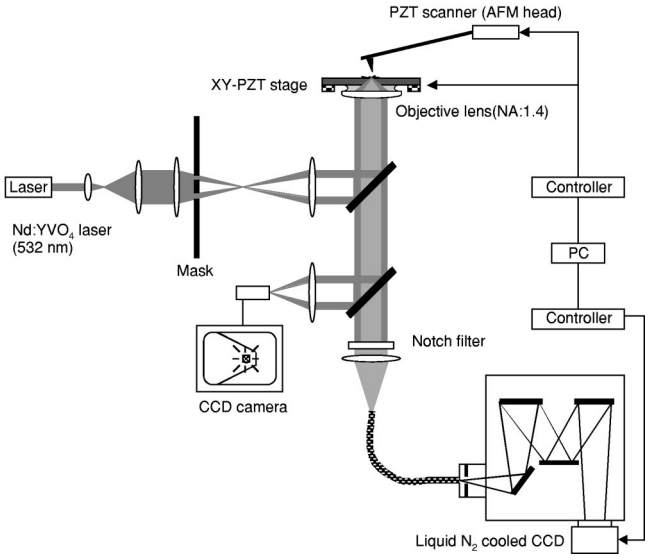

FIG. 2. Experimental setup of near-field Raman spectroscopy.

(CT) or chemical mechanism[48] that is one of the enhancement mechanisms[49,50] of SERS.[51–54] The CT complexes of metals, which are located at the apex of the metallic tip, might be formed with the adsorbed species at the surface in the tip-enhanced Raman spectroscopy.

In the first part of this study we describe the experimental results of the tip-enhanced near-field Raman spectroscopy of a single nanocrystal of DNA-base adenine molecules using a silver-coated apertureless probe of an atomic force microscope and assign the Raman bands on the basis of a previous report.[34] In the second part we analyze the detected tip-enhanced Raman bands in comparison with the bands obtained in the conventional SERS spectrum by performing high-level density-functional (DFT) calculations of the adenine complexes, including silver atoms.

II. TIP-ENHANCED NEAR-FIELD RAMAN SPECTRA OF ADENINE NANOCRYSTALS

For the tip-enhanced Raman NSOM experiments, we employed the same setup as described in our previous work.[25] The experimental setup is drawn in Fig. 2. The light source for the excitation of Raman scattering was a frequency-doubled Nd:YVO_4 laser, with an average power of about 2.5 mW, operating at a wavelength of 532 nm, at which adenine has negligible absorption. The probing laser beam was focused at the sample by an oil-immersion objective lens having a large numerical aperture (NA) equal to 1.4 and a magnification factor of 60. A portion of the incident beam with focusing angles equivalent to a NA less than 1.0 was truncated by a circular absorbing mask inserted at the light path to form an evanescent field light at the focused spot.[55] The Raman NSOM probe was an atomic force microscope (AFM) silicon cantilever coated with a 40-nm-thick silver layer by a thermal evaporation process. The evaporation rate was restricted to the relatively slow rate of 0.01 nm per second to obtain a smooth coating. The tip of the cantilever was set in 10 cm to the silver target, turning to the direction of the target. The silver-coated tip diameter was determined by a scanning electron microscope. Its typical value was 40 nm. The silver-coated cantilever was used at once for the experiment to avoid reducing the effectiveness of surface plasmons. We experimentally confirmed that the effectiveness lasted for one or two days. The distance between the sample and the metallic cantilever was controlled by the contact mode of the standard AFM operation. The scattered light was collected by the same objective lens, and directed to a spectrophotometer (the focal length is 300 mm, 1200 lines/mm) equipped with a liquid-nitrogen-cooled charge-coupled device (CCD) detector (1340×400 channels) for Raman spectra measurements. The excitation light and the scattered Rayleigh signal were sufficiently reduced using a holographic notch filter [the center wavelength is 532 nm, the full width at half maximum (FWHM) is 6 nm, and the optical density (OD) is greater than 6.0 at 532 nm].

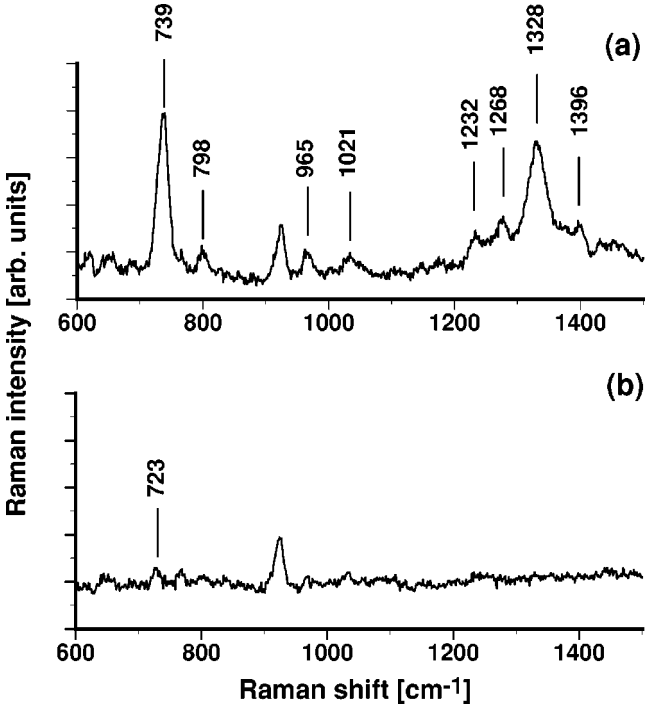

FIG. 3. (a) Tip-enhanced near-field Raman and (b) far-field Raman spectra of adenine nanocrystals. The peak at 923 cm^{-1} is derived from the glass substrate.

A. Preparation

Adenine was purchased from the Extrasynthese Co. and was not treated with any further purification. Adenine nanocrystals were prepared by casting an ethanol solution of adenine molecules (0.1 mmol/l) on a cover-glass slip. The size of the nanocrystals was about 7×20 nm in the lateral direction and 15 nm thick.

B. Raman NSOM experiments

Figure 3 shows Raman spectra measured using our system. The tip-enhanced Raman spectrum [Fig. 3(a)] of a single nanocrystal of adenine molecules was measured when

TABLE I. Vibrational frequencies of the tip-enhanced Raman (TERS) of adenine nanocrystals and assignment of theoretical frequencies to the experimental bands. The results of the SERS and normal Raman (NR) of adenine, calculated frequencies at the B3LYP functional using the 6-31++$G(d,p)$ basis set and theoretical assignment from McNaughton *et al.* (Ref. 34) are listed. Frequencies are given in cm^{-1}.

	This study	McNaughton *et al.*[a]				McNaughton *et al.*[a]
Band	TERS	SERS	NR	B3LYP	Plane	Assignment[b]
A	1401	1397	1419	1441	in	str C_4-N_9, C_4-C_5, C_6-N_{10}, N_7-C_8, bend C_2-H
B	1328	1336	1333	1372	in	bend C_2-H, C_8-H, N_9-H, str C_6-N_1, O_8-N_9, N_3-C_4
				1365	in	str C_5-N_7, N_1-C_2, bend C_2-H, C_8-H
C	1247	1268	1248	1272	in	bend C_8-H, N_9-H, str N_7-C_8
D	1232	1244	1234	1246	in	rock NH_2, str C_5-N_7, N_1-C_2, C_2-N_3
E	1021	1029	1025	1012	in	rock NH_2
F	965	961	942	942	in	def R5 (sqz group N_7-C_8-N_9)
G	798	790	797	805	out	def R6(wag C_4-C_5-C_6), wag C_8-H
H	739	733	723	726	in	ring breath whole molecule (distorted)

[a]Reference 34.

[b]Str; stretching; bend, bending; rock, rocking; def, deforming; wag, wagging; breath, breathing; R5, five-membered ring; R6, six-membered ring.

the silver-coated tip was in contact with the sample surface. Eight Raman bands, including two intense scattered bands at 739 or 1328 cm^{-1}, were detected. The peak at 924 cm^{-1} was due to the Raman scattering of the cover-glass slip. The far-field Raman spectrum [Fig. 3(b)] of the same sample using the same microscope, without the silver-coated tip, was shown to have almost no Raman scattering from the adenine molecule except for the faint band at 723 cm^{-1}. The measurement conditions were exactly the same for both experiments except for the tip-sample distance. Exposure time was set to 1 min for both measurements.

Table I shows the normal modes of the eight Raman bands that have been identified via the vibrational calculations reported by McNaughton *et al.*[34] The peak positions observed in the normal Raman spectrum of polycrystalline adenine[34] and in the SERS spectrum of adenine molecules adsorbed in colloidal silver[34] are listed together in the same table. The near-field Raman band at 739 cm^{-1} (band *H*) is assigned to a ring-breathing mode of whole adenine molecules. The band at 1328 cm^{-1} (band *B*) is assigned to a summation of two different vibrational modes. The first mode involves the C_5-N_7 and N_1-C_2 symmetric stretching coupled with the C_2-H and C_8-H symmetric in-plane bend. The second mode involves the C_2-H, C_8-H, and N_9-H in-plane bend with a minor contribution from the C_6-N_1, C_8-N_9, and N_3-C_4 stretches. The six other bands are also assigned to the corresponding internal vibrational modes of the adenine molecule. It is important to note that some of the eight bands detected in the silver-tip-enhanced near-field Raman spectrum for adenine nanocrystal apparently differ in the frequencies from the corresponding bands in the SERS for adenine adsorbed on colloidal silver. The band due to the ring-breathing mode at 739 cm^{-1} in the near-field Raman is 16 cm^{-1} higher than the Raman band of the ring-breathing mode in normal Raman. The band due to the same in SERS is at 733 cm^{-1}, which is only 10 cm^{-1} higher than in normal Raman spectra. It is widely reported[33–36,56] that the SERS spectra of adenine molecules depend on the substrate used. However, the SERS band due to the ring-breathing mode shows a shift to 733 cm^{-1} in colloidal silver,[34] 731 or 732 cm^{-1} in a silver electrode,[34,35] 732 cm^{-1} in vacuum-deposited silver-island film,[34] and 735 cm^{-1} in a silver nanoparticle,[56] against the band in the tip-enhanced Raman. These interesting phenomena suggest that the shifts of Raman frequencies caused by dynamic contacting of the silver-coated tip on the samples may differ from the shifts attributed to the surface enhancement effects caused by thermally stable adsorption of the samples onto the silver surfaces in the conventional SERS.

Figure 4(a) shows a spectral mapping of the tip-enhanced Raman spectra for nanocrystals of adenine molecules obtained using the silver-coated tip at 30-nm intervals in the near-field region on the focused spot using the AFM contact mode. The exposure time of the image is set to 10 s per line scan. Figure 4(b) exhibits intensity distributions of the two predominant Raman bands at 739 and 1328 cm^{-1}. The intensity distribution at 850 cm^{-1}, where no Raman band exists, shows no particular optical response signal in the same figure. The peak response at 60 nm of the *X* axis as well as the edge response of the intensity profile around 120 nm of the *X* axis in Fig. 4(b) suggests that the smallest observable feature is 30 nm. Assuming that the diameter of the enhanced electric field is 30 nm corresponding to the diameter of the lateral resolution and that the diameter of the focused light spot is 400 nm, the enhancement factor for the ring-breathing mode of the whole molecule at 739 cm^{-1} is 2.7×10^3. Furthermore, it is difficult to calculate the enhancement factor for the band at 1328 cm^{-1} because the far-field Raman signal without the tip is too weak to be detected. An enhancement factor of 10^3–10^4 observed in the silver-coated tip is reasonable compared to the SERS spectra of adenine molecules adsorbed on silver spheres having the same radii as the width of the probe tip apex (the excitation frequency is also the same).[57]

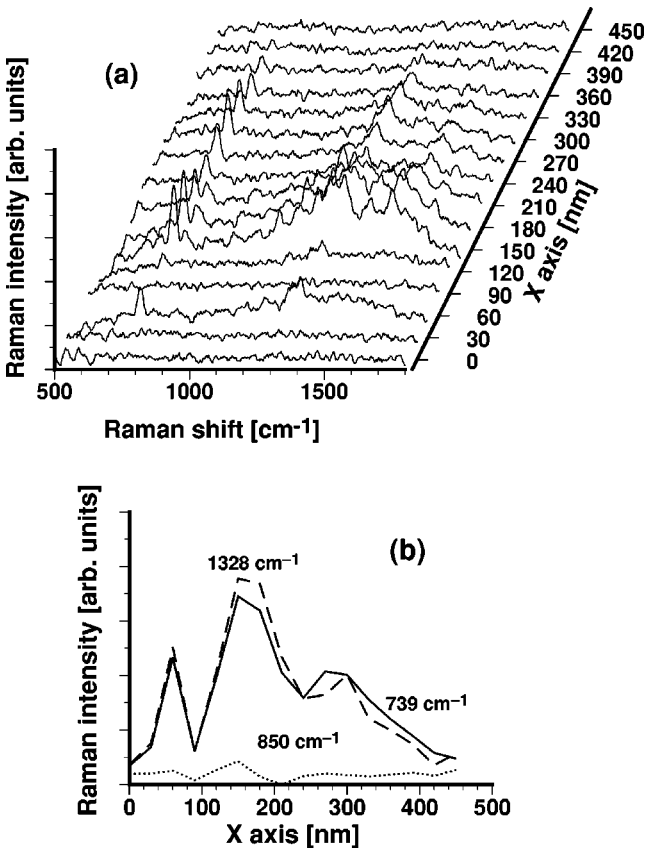

FIG. 4. (a) Near-field Raman spectral mapping of adenine nanocrystals at 30 nm intervals. Each spectrum is the subtraction of the corresponding tip-enhanced near-field Raman spectrum from the far-field Raman. (b) Raman intensity distributions of typical Raman bands at 739 and 1328 cm^{-1} against the tip displacement within the focused spot. The intensity distribution at 850 cm^{-1} is also given.

Other DNA bases, thymine, guanine, and cytosine, have their specific Raman bands due to the ring-breathing modes at 670, 681, 782 cm^{-1}, respectively.[58] A whole DNA sequence[57,59,60] can be identified directly by detecting such specific ring-breathing modes by the tip-enhanced near-field Raman spectroscopy without dye staining as compared to ordinary DNA sequencing methods, such as fluorescence *in situ* hybridization (FISH), where the spatial resolution is restricted by the diffraction limit. Spatial resolution required for the direct DNA sequencing could be around 0.3 nm (the distance between two adjacent bases in a helix strand), while the current smallest observable feature of the near-field Raman scattering is 30 nm.

III. VIBRATIONAL CALCULATIONS FOR FREQUENCY SHIFTS AFFECTED BY A METALLIC TIP

A. Quantum chemical approach

A quantum chemical study[61] for the Raman band shifts of pyridine molecules adsorbed on various metal surfaces was reported using density-functional theory (DFT) calculations, where a pyridine-metal (1:1) complex representing an appropriate adsorption model of pyridine molecules on the metals was discussed. Although this model is quite simple, the calculation results agree well with the SERS spectra of pyridine adsorbed on the corresponding metal surfaces. Especially in the case of the silver metal, the model complex was experimentally obtained in a solid argon matrix and exhibited whole vibrational frequencies similar to the SERS.[62] We employed this simple model to analyze the Raman band shifts of adenine and to calculate some adenine-silver metal (1:1) complexes.

Quantum chemical calculations to analyze and identify the vibrational frequencies, normal modes, and Raman intensities for free adenine molecule were carried out using the B3LYP functional[63,64] with the basis set of 6-311 $+G(d,p)$. The vibrational properties of the adenine-silver complexes were calculated using the UB3LYP functional in combination with the basis set of 6-311$+G(d,p)$ for carbon, nitrogen, or hydrogen atom, and the Stuttgart/Dresden relativistic effective core potentials combined with the associated basis functions of the valence electrons[65] (SDD) for a silver atom. The calculations were performed using the GAUSSIAN98 Revision A.9 program package.[66] Optimized ge-

TABLE II. Optimized bond lengths (in Å), bond angles (in degrees), dihedral angles (in degrees), and binding energies (in kilocalories per mole) of adenine at the B3LYP/6-311$+G(d,p)$ level and its silver complex isomers at the UB3LYP/6-311$+G(d,p)$ (for C, N, H/SDD) (for Ag) level.

	Adenine		Ad-N1	Ad-N3	Ad-N7	Ad-N10
Coordinate[a]	B3LYP	Crystal[b]	UB3LYP			
N-Ag			2.524	2.502	2.502	2.946
Ad-N-Ag[c]			0.7	0.0	0.1	−112.2
N_1-C_2	1.341	1.338	1.347	1.335	1.339	1.342
C_2-N_3	1.334	1.332	1.328	1.338	1.335	1.334
N_3-C_4	1.336	1.342	1.338	1.340	1.334	1.334
C_4-C_5	1.397	1.382	1.396	1.395	1.396	1.399
C_5-C_6	1.409	1.409	1.410	1.410	1.413	1.405
C_5-N_7	1.385	1.385	1.382	1.383	1.387	1.384
N_7-C_8	1.308	1.312	1.308	1.308	1.312	1.308
C_8-N_9	1.380	1.367	1.380	1.381	1.371	1.380
C_6-N_{10}	1.353	1.337	1.346	1.349	1.349	1.371
N_1-C_2-N_3	128.5	129.0	128.0	127.9	128.4	128.2
C_2-N_3C_4	111.5	110.8	111.7	112.4	111.4	111.7
N_3-C_4-C_5	126.7	126.9	126.7	125.9	126.9	126.6
C_4-C_5-C_6	116.0	116.9	116.4	116.3	116.1	115.8
C_4-C_5-N_7	111.3	110.7	111.3	111.0	110.4	111.2
C_5-N_7-C_8	104.2	103.9	104.2	104.3	105.0	104.2
N_7-C_8-N_9	113.2	113.8	113.2	113.2	112.6	113.3
C_5-C_6-N_{10}	122.3	123.4	122.6	122.4	123.1	122.3
N_1-C_6-N_{10}-H	0.0		−1.3	−0.5	−0.6	−19.4
ΔE			3.7	3.9	3.5	0.5
$\Delta(E+\mathrm{ZPE}^{d})$			3.2	3.4	3.0	−0.3

[a]Atom numbering as in Fig. 1.
[b]References 43 and 71.
[c]The angle between the plane of the purine ring and the bond axis of the silver atom and the adjacent nitrogen is given.
[d]The zero point energy (ZPE) is corrected by the scaled frequencies with a single factor of 0.989 (Ref. 70).

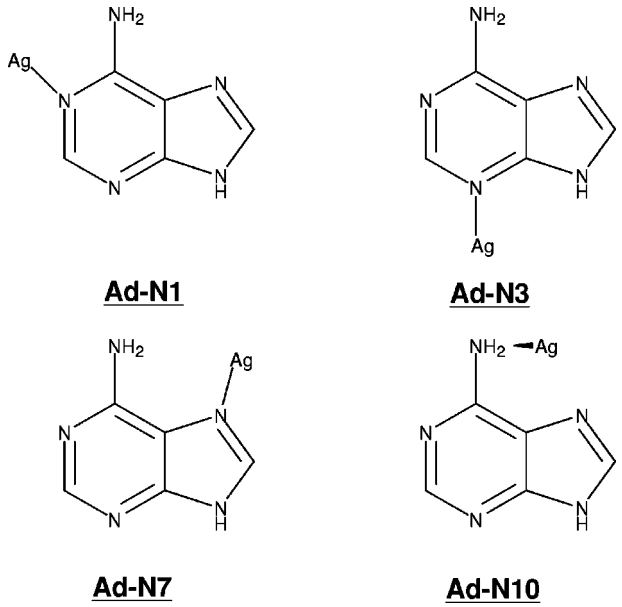

FIG. 5. Molecular structure of four adenine-silver complex isomers.

ometries and the calculated vibrational modes were visualized using the MOLDEN program[67] (QCPE 619) and the VLX program,[68] respectively.

B. Vibrational calculation of adenine molecule

The vibrational frequencies and the Raman intensities have been calculated using DFT calculations for adenine and its silver complexes, in order to analyze the frequency shifts of Raman bands of adenine affected by the silver-coated tip. The geometrical structure of the adenine molecule was optimized at the B3LYP functional using the $6\text{-}311+G(d,p)$ basis set, which was then followed by calculations of the vibrational properties at the same level of theory using the same basis set. The calculated geometrical parameters are listed in the left side of Table II with results from the crystallographic structure of adenine.[69] The calculated bond lengths and bond angles agree well with the crystallographic structure. The predicted geometry is a planar shape (C_S symmetry) having no imaginary frequencies, representing an energy minimum. This geometry slightly differs from the results reported by McNaughton *et al.*[34] They reported that the optimized geometry was nonplanar with the hydrogens of the amino group located slightly above the plane of the purine ring (C_1 symmetry) at the B3LYP functional using the $6\text{-}31++G(d,p)$ basis set. The geometry of the adenine molecule depends on the basis set used in the theoretical model. It can be interpreted that this basis set dependency is due to a shallow potential surface in the out-of-plane coordinate for the two hydrogen atoms of the external amino group. Multiplying the calculated vibrational frequencies by a single scale factor of 0.9942 provides a good fit between the calculated and the observed frequencies. In spite of the differences in the calculated geometries of the adenine molecule, our calculated results of vibrational properties are substantially the same as those reported by McNaughton *et al.*[34]

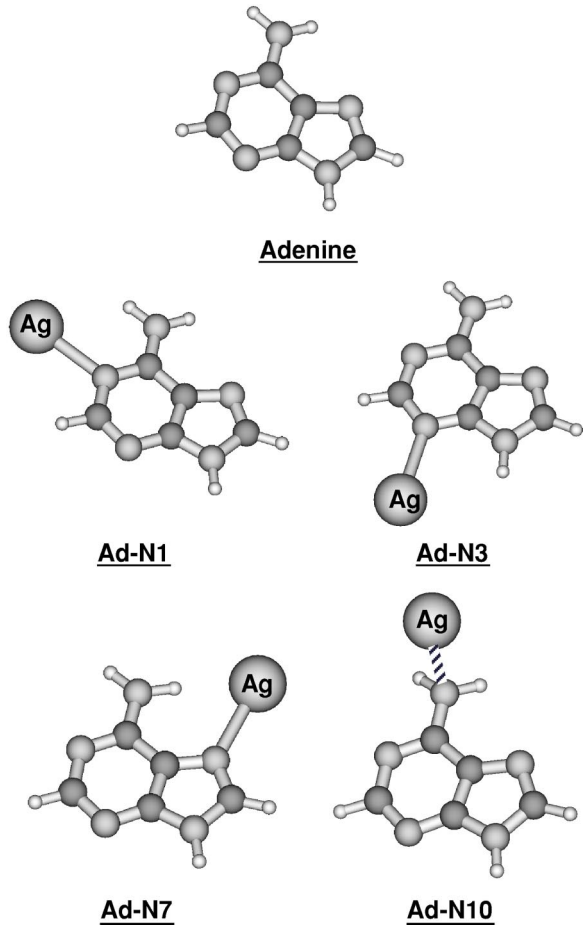

FIG. 6. Optimized geometry of adenine molecule and its silver complex isomers.

C. Vibrational calculation of adenine silver complexes

Four possible adenine-silver complex isomers were examined in which every silver atom is adjacent to any position of nitrogen atoms at N_1, N_3, N_7, and N_{10}, respectively. Complex isomers in which a silver atom is adjacent to N_9 nitrogen of the N_7-H adenine tautomer were omitted because of the instability of the N_7-H tautomer.[43] These four isomers are the simplest models having the interaction of adenine with the silver metal surface and the silver-coated tip at the apex. The structures of the Ad-N1, Ad-N3, Ad-N7, and Ad-N10 isomers are illustrated in Fig. 5. The geometries of these isomers were fully optimized with the UB3LYP functional using the same basis set for adenine moiety and the SDD pseudopotentials for silver. The vibrational properties were then calculated using the same level of the DFT calculations and basis set conditions. The spin states for these isomers are doublet and the charges are neutral for all. The calculated geometrical parameters are listed in Table II, which also contains the calculated relative binding energies (ΔE) corrected with the zero-point energies (ZPE) based on a scaled harmonic normal-mode frequency with a single factor of 0.989.[70] The optimized geometries of the adenine molecule and four complex isomers are demonstrated in Fig. 6, which represent energy minima due to the absence of imaginary

TABLE III. Calculated vibrational frequencies, Raman intensities of adenine at the B3LYP/6-311 $+G(d,p)$ level and its silver complex isomers at the UB3LYP/6-311$+G(d,p)$ (for C, N, H)/SDD (for Ag) level. Vibrational frequencies scaled by a single factor of 0.9942 are given. Raman activities are given in units of $Å^4\,amu^{-1}$.

	Adenine		Ad-N1		Ad-N3		Ad-N7		Ad-N10	
Mode	ν/cm^{-1}	Intensity	ν/cm^{-1}	Intensity	ν/cm^{-1}	Intensity	ν/cm^{-1}	Intensity	ν/cm^{-1}	Intensity
1	1647	9.1	1654	18.6	1651	27.6	1652	13.3	1638	7.6
2	1625	21.9	1621	24.4	1624	19.8	1625	18.0	1629	27.8
3	1599	4.6	1598	19.6	1603	5.5	1601	15.5	1601	15.6
4	1505	77.1	1504	134.1	1506	52.4	1510	86.4	1505	95.3
5	1493	13.0	1497	0.6	1492	29.1	1493	35.0	1488	19.8
6	1424	0.6	1429	10.2	1433	11.0	1425	4.2	1419	5.0
7	1406	27.3	1406	41.4	1412	36.0	1411	33.4	1406	29.0
8	1356	39.1	1362	57.4	1357	32.7	1358	21.0	1352	99.6
9	1348	36.3	1347	35.0	1359	54.0	1352	33.4	1344	37.7
10	1319	17.9	1331	39.0	1318	23.7	1317	13.1	1315	68.3
11	1259	16.8	1258	22.5	1259	58.0	1259	32.9	1259	14.5
12	1235	15.5	1238	23.2	1237	25.6	1232	1.8	1246	24.6
13	1136	2.5	1140	2.6	1141	6.7	1136	3.8	1133	4.9
14	1073	8.5	1073	10.3	1072	22.1	1092	3.0	1073	7.9
15	1003	5.0	1007	23.4	1005	5.2	1009	3.2	1032	10.5
16	970	0.1	968	1.4	968	0.3	975	0.1	970	1.1
17	939	4.2	941	6.9	942	4.4	951	4.8	938	6.0
18	895	1.7	901	3.6	903	0.6	895	0.9	894	3.0
19	846	1.0	850	1.4	853	0.5	849	0.0	854	3.3
20	804	0.6	799	0.1	799	0.5	799	0.1	807	8.9
21	721	25.3	721	30.5	724	49.6	721	36.8	721	23.7
22	681	0.2	679	0.2	679	0.1	681	0.2	681	25.7
23	663	0.2	662	1.5	664	0.3	660	0.6	662	1.5
24	615	7.2	623	15.5	615	4.6	616	5.0	619	7.5
25	572	0.7	572	0.9	574	4.2	572	1.0	574	3.4
26	536	0.0	545	5.3	547	0.1	546	6.4	537	7.7
27	529	3.2	532	3.3	535	10.7	529	4.3	555	8.8
28	517	2.8	522	3.0	522	2.4	521	4.8	523	4.1
29	514	0.9	523	0.3	535	4.1	524	1.3	515	3.4
30	297	0.0	296	0.6	301	0.3	299	0.2	300	2.4
31	275	3.0	283	4.0	277	2.4	301	5.5	496	1.0
32	215	0.0	214	5.1	224	0.2	202	1.5	217	0.2
33	163	0.2	158	0.2	188	0.1	158	0.4	172	12.7
34	51	0.0	222	5.7	157	0.3	248	11.1	273	2.5
35			79	2.9	85	4.4	90	4.9	47	27.2
36			67	0.7	51	0.8	66	0.0	28	3.4
37			30	5.5	40	5.3	37	4.7	25	1.0

frequencies. In our calculation level, the most stable isomer is the Ad-N3, where the silver atom is located along the plane of the purine ring and two hydrogen atoms that are slightly above the plane (C_1 symmetry). The calculated binding energies of the other isomers were nearly equal or slightly higher by only a few kilocalories per mole, with or without the ZPE correction. This means that these four adenine-silver complex isomers are probable candidates for the interaction models as far as the binding energies are concerned. Both the Ad-N1 and the Ad-N7 exhibit geometrical characteristics similar to the Ad-N3. These three isomers demonstrate a ''side-on'' adsorption to silver surfaces. In the geometry of the Ad-N10, the silver atom is located above the plane in contrast with the other isomers. This configuration represents the simplest model of a ''flat-on'' adsorption onto silver surfaces.

The calculated frequencies of these isomers were uniformly scaled by the same factor of 0.9942 as employed in a free adenine molecule. The corrected vibrational frequencies vs the Raman intensities of an adenine molecule and its iso-

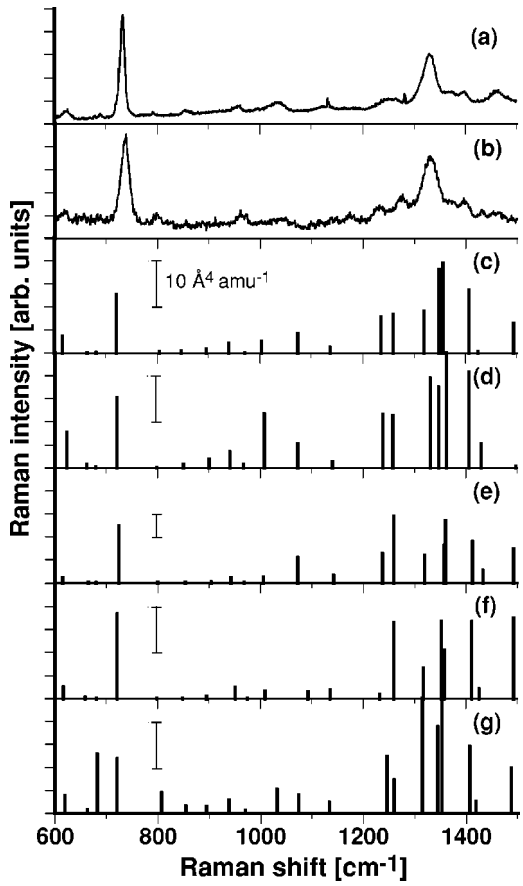

FIG. 7. (a) The SERS spectrum of adenine molecules adsorbed on colloidal silver. (b) The tip-enhanced near-field Raman spectrum of adenine nanocrystals. The predicted Raman spectra of (c) adenine and its silver complex isomers: (d) Ad-N1, (e) Ad-N3, (f) Ad-N7, and (g) Ad-N10, as synthesized from the calculated Raman intensities against the corresponding frequencies.

mers are listed in Table III. This does not include the results relating to the CH stretching modes having frequencies higher than 3000 cm^{-1}. Figure 7 shows the SERS spectrum of adenine adsorbed on colloidal silver, the tip-enhanced near-field Raman spectrum of an adenine nanocrystal, and the predicted Raman spectra, which are plotted versus the corresponding frequencies in the region of 1500 to 600 cm^{-1}.

D. Comparison between the calculated and measured Raman spectra

Comparing with the SERS spectrum of Fig. 7(a), there are some spurious Raman bands in the calculated Raman spectra of both the Ad-N1 and the Ad-N10. The calculated Raman spectrum of the Ad-N1 [Fig. 7(d)] involves a strong band at 1007 cm^{-1} due to the N_{10}-H in-plane rocking mode (ν_{15} in Fig. 8), while no significant Raman peaks in this frequency region are observed for the SERS spectrum. The calculated spectrum of the Ad-N10 in Fig. 7(g) exhibits two strong bands at 807 cm^{-1} and 681 cm^{-1} due to the out-of-plane ring-deforming modes (ν_{20} and ν_{22}, respectively in Fig. 8), while no corresponding peaks exist in the frequency regions

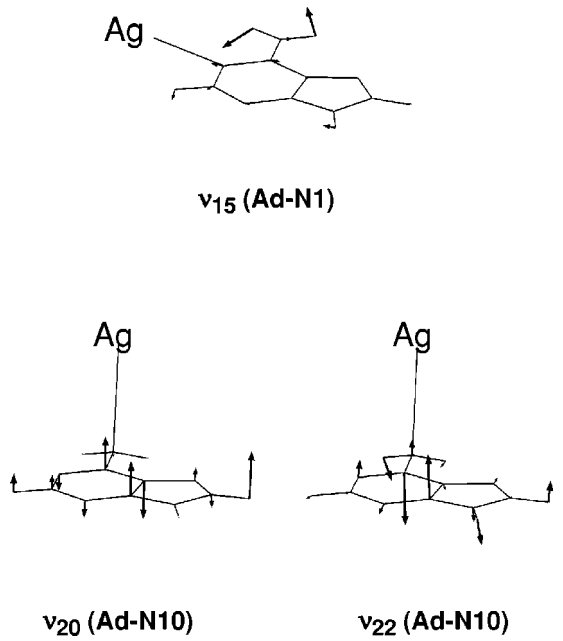

FIG. 8. Vibrational patterns of some normal modes for adenine-silver complex isomers. The mode number is given to each mode of the isomers.

of the SERS spectrum. From the results, these two isomers do not seem to be active species of SERS. The calculated Raman spectra of both the Ad-N3 [Fig. 7(e)] and the Ad-N7 [Fig. 7(f)] agree relatively well with the SERS spectrum. The calculated Raman band due to the ring-breathing mode (ν_{21}) of the Ad-N3 shows a higher frequency shift by 3 cm^{-1} to the calculated band of free adenine [shown in Fig. 7(c)], which coincides with the experimental data observed in SERS. In contrast, the same bands of the Ad-N7 show no frequency shift. These results show that the Raman active species observed in SERS have the structure of adenine molecules adsorbed on the silver surfaces via N_3 nitrogen (Ad-N3). The Ad-N3 model therefore best represents the structure; however, it is not easy to differentiate between the two isomers from such a small frequency shift.

In comparison with the tip-enhanced near-field Raman spectrum [Fig. 7(b)], there are also the unclear Raman bands in the calculated Raman spectra of both the Ad-N1 and the Ad-N10 isomers. Neither of these two isomers are active species in the tip-enhanced Raman NSOM for the same reasons. Although whole spectral patterns of the calculated Raman spectra of both the Ad-N3 and the Ad-N7 are similar to that of the tip-enhanced near-field Raman spectrum, the large frequency shift of the tip-enhanced near-field Raman band towards high frequency due to the ring-breathing mode at 739 cm^{-1} does not appear in the calculated spectra of either the Ad-N3 or the Ad-N7.

E. Deformation of adenine molecules due to the atomic force of silver atoms at the metallic tip

One of the major differences in the experimental conditions between the tip-enhanced Raman NSOM from those of the SERS spectroscopy is due to the form of adenine mol-

TABLE IV. Calculated relative binding energies (ΔE), and vibrational frequencies of adenine at the B3LYP/6-311+$G(d,p)$ level and its silver complex isomers at the UB3LYP/6-311+$G(d,p)$ (for C, N, H)/SDD (for Ag) level against the bond distances of Ag-N (in Å). Energy units are kilocalories per mole. Frequencies scaled by a single factor of 0.9942 are given. Raman activities are given in units of $Å^4\,amu^{-1}$.

	Adenine	Ad-N3				Ad-N7			
Ag-N		2.75	2.50	2.25	2.00	2.75	2.50	2.25	2.00
ΔE	0	3.4	3.9	2.2	−7.8	2.7	3.5	1.8	−7.3
Mode		Wave number/cm^{-1}							
1	1647	1650	1651	1653	1656	1650	1652	1652	1652
2	1625	1624	1624	1623	1619	1624	1625	1625	1624
3	1599	1602	1603	1605	1607	1601	1601	1598	1595
4	1505	1505	1506	1507	1509	1508	1510	1512	1516
5	1493	1492	1492	1491	1488	1493	1492	1491	1490
6	1424	1430	1433	1435	1437	1425	1425	1427	1429
7	1406	1409	1412	1415	1419	1409	1411	1414	1419
8	1356	1357	1357	1357	1357	1358	1358	1358	1358
9	1348	1356	1359	1364	1370	1350	1352	1352	1351
10	1319	1319	1318	1314	1303	1318	1317	1315	1310
11	1259	1259	1259	1258	1256	1259	1259	1259	1256
12	1235	1236	1237	1236	1233	1232	1232	1230	1232
13	1136	1139	1142	1146	1158	1135	1136	1137	1143
14	1073	1070	1072	1071	1071	1086	1092	1099	1106
15	1003	1005	1005	1006	1006	1008	1009	1010	1019
16	970	968	968	967	964	974	975	977	978
17	939	941	942	943	943	945	951	964	995
18	895	899	903	915	952	895	895	895	895
19	846	852	853	855	857	847	849	850	848
20	804	800	799	798	796	800	799	797	796
21	721	722	724	729	741	721	721	721	725
22	681	680	679	679	677	681	681	681	681
23	663	664	664	665	665	660	660	657	654
24	615	615	615	615	617	615	616	619	627
25	572	572	574	575	577	571	572	572	573
26	536	544	542	550	552	542	546	548	552
27	529	531	535	543	563	528	529	529	533
28	517	520	522	524	526	519	521	522	524
29	514	529	535	539	541	520	524	527	530
30	297	300	301	298	294	298	299	300	303
31	275	276	277	279	285	293	301	302	307
32	215	220	224	234	250	156	158	159	257
33	163	175	188	199	201	229	249	271	287
34	51	149	157	158	231	193	202	205	205
35		43	85	149	157	54	90	154	145
36		41	51	66	47	35	66	70	51
37		35	40	54*i*	103*i*	28	37	35*i*	97*i*

ecules: a unimolecular form in the SERS spectroscopy and a nanocrystalline form in the tip-enhanced Raman NSOM. However, this difference is not the dominant cause of a change in the frequency because there are no significant frequency shifts observed when comparing IR frequencies of matrix-isolated adenine[46] with IR and Raman frequencies of crystalline adenine.[34] The other difference in experimental conditions is the interaction mechanism of adenine with silver surfaces. In SERS, adenine is adsorbed in equilibrium onto silver surfaces, whereas in the tip-enhanced Raman NSOM, nanocrystalline adenine is pressed by the silver probe tip with a constant atomic force. Assuming that the atomic force is applied only to the contraction of the bond between the silver atom of the tip and the adjacent nitrogen of the adenine molecule, the bond distance would be expected to shrink and the vibrational frequencies may then shift. In our experiment, we used a cantilever with a spring constant of 0.03 N/m and a silver-coated tip apex diameter of

this cantilever was 5–10 nm. The atomic force was kept constant at 0.3 nN by the feedback loop. Deduced from the unit-cell parameters of single-crystal 9-methyladenine,[71] a couple of adenine molecules exists in a rectangle approximately 0.77 nm lateral by 0.85 nm wide. If we assume that the force is equally applied to all the molecules which are adjacent to the tip apex, the adenine molecules are subjected to a pressure of ~1–5 pN/molecule by the silver atom attached on the surface of the tip. For the further understanding of the tip-enhanced near-field Raman active species of adenine molecules, we investigated the transition states of both the Ad-N3 and the Ad-N7 isomers by changing the bond distance (in the model) between the nitrogen of adenine molecule and the silver atom. The bond distances for the calculations were 2.502 (equilibrium), 2.75 (10% elongation), 2.25 (10% contraction), and 2.0 Å (20% contraction). The binding energies (ΔE), the vibrational frequencies of free adenine molecules, and the two complex isomers of three states are calculated as shown in Table IV. The results relating to the CH stretching modes having frequencies higher than 3000 cm^{-1} are omitted. The partially optimized geometries exhibit imaginary frequencies, indicating transition states for the Ad-N3 and the Ad-N7. The calculated frequency shifts of the Raman bands having the highest intensities (ν_8 and ν_{21} in Table IV) in the tip-enhanced Raman NSOM and the calculated potential curves are plotted as a function of the bond distance in Fig. 9. As for the rest of the six bands observed in the Raman NSOM, it is difficult to analyze the frequency shifts quantitatively because the signal-to-noise ratio of these bands is not sufficient for the analysis.

As the metallic tip of the cantilever approaches the surface of the adenine nanocrystal, the tip is at first subject to a van der Waals attractive force and after passing through the equilibrium point, the tip receives a repulsive force. In our experiment, the atomic force which is balanced with the repulsive force is set at 1–5 pN/molecule as described before. When the bond distance of the Ag-N linkage is reduced by 10%, the repulsive force of 7 pN/molecule is derived from a harmonic oscillation of the displacement by 0.025 nm and the energy difference by 1.7 kcal/mol in the case of the Ad-N3. The repulsive force coincides with the atomic force obtained with our system.

The ring breathing mode ν_{21} of the Ad-N3 shows a significant shift towards a higher frequency as a function of the contracted bond distance between the silver atom and the N_3 nitrogen of adenine. The frequency of the ν_{21} mode is shifted upwards by 5 cm^{-1} when the bond distance is reduced by 10%. The frequency is shifted upwards by 17 cm^{-1} when the bond distance is reduced by 20%. In contrast, the calculated frequency shift of the other band (ν_8 in Fig. 9) of the Ad-N3 is very small. The frequency shifts of these two bands agree with those of the bands obtained by the tip-enhanced Raman NSOM. On the other hand, the Ad-N7 shows only small frequency shifts for both of these two bands in Fig. 9. These differences in frequency shifts suggest that interaction between an adenine molecule and the silver tip (e.g., the Ad-N3) may be one of the possible reasons that we see large enhancement effects in the tip-enhanced Raman NSOM.

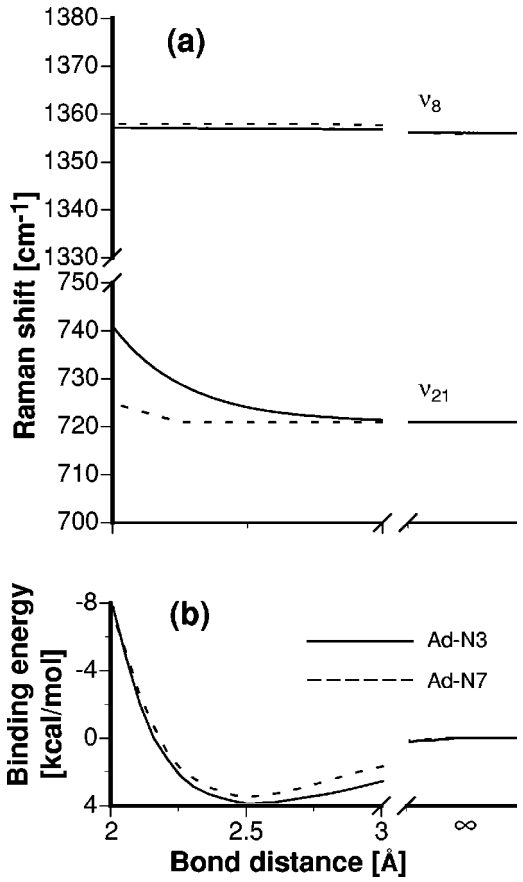

FIG. 9. (a) The calculated frequency shifts of two Raman bands (ν_8 and ν_{21}) of the Ad-N3 and the Ad-N7 and (b) the calculated binding energies as a function of the bond distance for the Ag-N linkage.

In addition to the higher frequency shift, Raman band broadening is also observed in the tip-enhanced Raman spectra. The line broadening as well as the Raman frequency shift have been well reported in the high-pressure induced Raman spectroscopy.[72–74] Our tip-enhanced Raman spectra caused by the pressurized tip could be thought to observe the phenomenon which was similar to high-pressure Raman study. The line broadening occurs not only as a result of surface interaction, but also as a result of pressures caused by the silver tip.

While the quantum chemical vibrational calculation can provides quantitative estimates of frequency shifts, its accuracy is dependent on the physical model. Here, we treated the silver tips as a simple atom, leading to some discrepancies between the calculation and the experiment. More practical models are required for getting a precise picture. For example, it has been reported that a cluster of four silver spheres provides a gigantic magnification of the electromagnetic field.[75] Silver ions have also shown a significant shift to higher frequency in the ring breathing mode of pyridine.[61]

IV. CONCLUSION

Near-field Raman spectra of adenine nanocrystals have been successfully measured using the local field-

enhancement effect at the metallic tip. The smallest observable feature reaches 30 nm that exceeds the diffraction limit of the light. The intensity of Raman signals is amplified by a factor of more than 2.7×10^3 times compared with the far-field Raman intensity. The tip-enhanced near-field Raman spectra of adenine partially differs from the conventional SERS in vibrational frequencies. By means of normal mode analysis using the DFT calculations, we obtained vibrational frequency shifts for the transient states of the adenine-silver metal complexes. The calculated Raman spectra of the complexes could be made to agree with the tip-enhanced near-field Raman spectra of adenine by reducing the bond distance. Repulsive forces calculated from the reduction of the bond distance between adenine and the silver atom were equal to the atomic force applied to the adenine molecule in our Raman NSOM experiment. All results support that the active Raman shift occurs owing to the deformation of adenine molecules by the silver atoms of the metallic tip. In particular, the silver atoms presumably pressed against the N_3 nitrogen of the adenine molecules. The phenomenon of shifting near-field Raman spectra caused by pushing molecules with AFM is used for spectroscopic instrumentation of molecular analysis and identification at the nanoscale. Spatial resolution of our proposed method should be given by AFM which perturbs individual molecules. Hence the technique has the possibility of achieving molecular resolution in vibrational spectroscopy, such as short fragments of DNA sequencing lying flat on a surface.

ACKNOWLEDGMENTS

The authors gratefully acknowledge Dr. Prabhat Verma and Dr. Nicholas Smith for their valuable comments and discussions on this work.

*Author to whom correspondence should be addressed. Electronic address: ya-inoue@ap.eng.osaka-u.ac.jp

[1] D. W. Pohl, W. Denk, and M. Lanz, Appl. Phys. Lett. **44**, 651 (1984).
[2] A. Harootunian, E. Betzig, M. Isaacson, and A. Lewis, Appl. Phys. Lett. **49**, 674 (1986).
[3] E. Betzig and R. J. Chichester, Science **262**, 1422 (1993).
[4] X. S. Xie and R. C. Dunn, Science **265**, 361 (1994).
[5] W. P. Ambrose, P. M. Goodwin, J. C. Martin, and R. A. Keller, Science **265**, 364 (1994).
[6] D. P. Tsai, A. Othonos, M. Moskovits, and D. Uttamchandani, Appl. Phys. Lett. **64**, 1768 (1994).
[7] C. L. Jahncke, M. A. Paesler, and H. D. Hallen, Appl. Phys. Lett. **67**, 2483 (1995).
[8] D. A. Smith, S. Webster, M. Ayad, S. D. Evans, D. Fogherty, and D. Batchelder, Ultramicroscopy **61**, 247 (1995).
[9] S. Webster, D. N. Batchelder, and D. A. Smith, Appl. Phys. Lett. **72**, 1478 (1998).
[10] S. R. Emory and S. Nie, Anal. Chem. **69**, 2631 (1997).
[11] (a) D. Zeisel, V. Deckert, R. Zenobi, and T. Vo-Dinh, Chem. Phys. Lett. **283**, 381 (1988); (b) V. Deckert, D. Zeisel, R. Zenobi, and T. Vo-Dinh, Anal. Chem. **70**, 2646 (1998).
[12] S. L. Sharp, R. J. Warmack, J. P. Goudonnet, I. Lee, and T. L. Ferrell, Acc. Chem. Res. **26**, 377 (1993).
[13] Y. Inouye, N. Hayazawa, K. Hayashi, Z. Sekkat, and S. Kawata, in *Proceedings of SPIE, Denver, 1999*, edited by S. Jutamulia, M. Ohtsu, and T. Asakura (University of Denver, Denver, CO, 1999), Vol. 3791, p. 40.
[14] N. Hayazawa, Y. Inouye, Z. Sekkat, and S. Kawata, Opt. Commun. **183**, 333 (2000).
[15] R. M. Stockle, Y. D. Suh, V. Deckert, and R. Zenobi, Chem. Phys. Lett. **318**, 131 (2000).
[16] M. S. Anderson, Appl. Phys. Lett. **76**, 3130 (2000).
[17] L. T. Nieman, G. M. Krampert, and R. E. Martinez, Rev. Sci. Instrum. **72**, 1691 (2001).
[18] A. Hartschuh, E. J. Sanchez, X. S. Xie, and L. Novotny, Phys. Rev. Lett. **90**, 095503 (2003).
[19] J. Wessel, J. Opt. Soc. Am. B **2**, 1538 (1985).
[20] U. Ch. Fischer and D. W. Pohl, Phys. Rev. Lett. **62**, 458 (1989).
[21] H. Furukawa and S. Kawata, Opt. Commun. **148**, 221 (1998).
[22] L. Novotny, E. J. Sanchez, and X. S. Xie, Ultramicroscopy **71**, 21 (1998).
[23] J. Jersh, F. Demming, L. J. Hildenhagen, and K. Dickmann, Appl. Phys. A: Mater. Sci. Process. **66**, 29 (1998).
[24] R. K. Chang and T. E. Furtak, *Surface Enhancement Raman Scattering* (Plenum, New York, 1982).
[25] N. Hayazawa, Y. Inouye, Z. Sekkat, and S. Kawata, Chem. Phys. Lett. **335**, 369 (2001).
[26] N. Hayazawa, Y. Inouye, Z. Sekkat, and S. Kawata, J. Chem. Phys. **117**, 1296 (2002).
[27] N. Hayazawa, A. Tarum, Y. Inouye, and S. Kawata, J. Appl. Phys. **92**, 6983 (2002).
[28] Y. Inouye and S. Kawata, Opt. Lett. **19**, 159 (1994).
[29] R. Bachelot, P. Gleyzes, and A. C. Boccara, Opt. Lett. **20**, 1924 (1995).
[30] J. Koglin, U. Ch. Fischer, and H. Fuchs, Phys. Rev. B **55**, 7977 (1997).
[31] B. Knoll and F. Keilmann, Nature (London) **399**, 134 (1999).
[32] *Near-field Optics and Surface Plasmon Polariton*, edited by S. Kawata (Springer-Verlag, Berlin, 2001).
[33] S. K. Kim, T. H. Joo, S. W. Suh, and M. S. Kim, J. Raman Spectrosc. **17**, 381 (1986).
[34] B. Giese and D. J. McNaughton, J. Phys. Chem. B **106**, 101 (2002).
[35] (a) C. Otto, T. J. J. van den Tweel, F. F. M. de Mul, and J. Greve, J. Raman Spectrosc. **17**, 289 (1986); (b) C. Otto, F. F. M. de Mul, A. Huizinga, and J. Greve, J. Phys. Chem. **92**, 1239 (1988).
[36] T. Watanabe, O. Kawanami, H. Katoh, K. Honda, Y. Nishimura, and M. Tsuboi, Surf. Sci. **158**, 341 (1985).
[37] E. Koglin, J. M. Sequaris, and P. Valenta, J. Mol. Struct. **60**, 421 (1980).
[38] K. Itoh, K. Minami, T. Tsujino, and M. Kim, J. Phys. Chem. **95**, 1339 (1991).
[39] M. Majoube, J. Raman Spectrosc. **16**, 98 (1985).
[40] Z. Dhaouadi, M. Ghomi, J. C. Austin, R. B. Girling, R. E. Hester, P. Mojzes, L. Chinsky, P. Y. Turpin, C. Coulombeau, H. Jobic, and J. Tomkinson, J. Phys. Chem. **97**, 1074 (1993).
[41] G. N. Ten, V. V. Neckaev, V. L. Berezin, and V. I. Baranov, Zh. Strukt. Khim. **38**, 324 (1997) [J. Struct. Chem. **38**, 262 (1997)].

[42] J. Florian, J. Mol. Struct.: THEOCHEM **253**, 83 (1992).
[43] J. Wiorkiewicz-Kuczera and M. Karplus, J. Am. Chem. Soc. **112**, 5324 (1990).
[44] M. Majoube, Ph. Millie, P. Lagant, and G. Vergoten, J. Raman Spectrosc. **25**, 821 (1994).
[45] (a) M. J. Nowak, H. Rostkowska, L. Lapinski, J. S. Kwiatkowski, and J. Leszczynski, Spectrochim. Acta **50A**, 1081 (1994); (b) M. J. Nowak, H. Rostkowska, L. Lapinski, J. S. Kwiatkowski, and J. Leszczynski, J. Phys. Chem. **98**, 2813 (1994).
[46] M. J. Nowak, L. Lapinski, J. S. Kwiatkowski, and J. Leszczynski, J. Phys. Chem. **100**, 3527 (1996).
[47] R. Santamaria, E. Charro, A. Zacarias, and M. Castro, J. Comput. Chem. **20**, 511 (1999).
[48] (a) A. Otto, J. Timper, J. Billman, G. Kovacs, and I. Pockrand, Surf. Sci. **92**, L55 (1980); (b) J. Billman, G. Kovacs, and A. Otto, *ibid.* **92**, 153 (1980); (c) A. Otto, J. Billmann, J. Eickmans, U. Ertuerk, and C. Pettenkofer, *ibid.* **138**, 319 (1984).
[49] The other important mechanism of the SERS is the electromagnetic (EM) enhancement mechanism. Theoretical evaluation of the enhancement factor of SERS spectra was reported using the electromagnetic analysis for the resolution of electrostatic, dispersive, and repulsive contributions in Ref. 50. However, frequency shifts of the spectra cannot be explained by this analysis.
[50] (a) S. Corni and J. Tomasi, Chem. Phys. Lett. **342**, 135 (2001); (b) S. Corni and J. Tomasi, J. Chem. Phys. **114**, 3739 (2001); (c) S. Corni and J. Tomasi, *ibid.* **116**, 1156 (2002).
[51] (a) F. W. King, R. P. Van Duyne, and G. C. Schatz, J. Chem. Phys. **69**, 4472 (1978); (b) S. Efrima and H. Metiu, *ibid.* **70**, 1939 (1979).
[52] J. A. Creighton, Surf. Sci. **124**, 209 (1983).
[53] M. Moskovits, Rev. Mod. Phys. **57**, 783 (1985).
[54] A. Campion and P. Kambhampati, Chem. Soc. Rev. **27**, 241 (1998).
[55] N. Hayazawa, Y. Inouye, and S. Kawata, J. Microsc. **194**, 472 (1999).
[56] K. Kneipp, H. Kneipp, V. B. Kartha, R. Manoharan, G. Deinum, I. Itzkan, R. R. Dasari, and M. S. Feld, Phys. Rev. E **57**, 6281 (1998).
[57] M. Kerker, D. S. Wang, and H. Chew, Appl. Opt. **19**, 4159 (1980).
[58] H. Deng, V. A. Bloomfield, J. M. Benevides, and G. J. Thomas, Jr., Biopolymers **50**, 656 (1999).
[59] W. A. Lyon and S. Nie, Anal. Chem. **69**, 3400 (1997).
[60] K. Kneipp, H. Kneipp, I. Itzkan, R. R. Dasari, and M. S. Feld, Chem. Rev. (Washington, D.C.) **99**, 2957 (1999).
[61] D. Y. Wu, B. Ren, Y. X. Jiang, X. Xu, and Z. Q. Tian, J. Phys. Chem. A **106**, 9042 (2002).
[62] W. Krasser, U. Kettler, and P. S. Bechthold, Chem. Phys. Lett. **86**, 223 (1982).
[63] A. D. Becke, J. Chem. Phys. **98**, 5648 (1993).
[64] C. Lee, W. Yang, and R. G. Parr, Phys. Rev. B **37**, 785 (1988).
[65] (a) P. Fuentealba, H. Preuss, H. Stoll, and L. v. Szentpaly, Chem. Phys. Lett. **89**, 418 (1982); (b) M. Kaupp, P. v. R. Schleyer, H. Stoll, and H. Preuss, J. Chem. Phys. **94**, 1360 (1991); (c) T. Leininger, A. Nicklass, H. Stoll, M. Dolg, and P. Schwerdtfeger, *ibid.* **105**, 1052 (1996).
[66] M. J. Frisch, G. W. Trucks, H. B. Schlegel, G. E. Scuseria, M. A. Robb, J. R. Cheesemann, V. G. Zakrzewski, J. A. Montgomery, Jr., R. E. Stratmann, J. C. Burant, S. Dapprich, J. M. Millam, A. D. Daniels, K. N. Kudin, M. C. Strain, O. Farkas, J. Tomasi, V. Barone, M. Cossi, R. Cammi, B. Mennucci, C. Pomelli, C. Adamo, S. Clifford, J. Ochterski, G. A. Petersson, P. Y. Ayala, Q. Cui, K. Morokuma, D. K. Malick, A. D. Rabuck, K. Raghavachari, J. B. Foresman, J. Cioslowski, J. V. Ortiz, A. G. Baboul, B. B. Stefanov, G. Liu, A. Liashenko, P. Piskorz, I. Komaromi, R. Gomperts, R. L. Martin, D. J. Fox, T. Keith, M. A. Al-Laham, C. Y. Peng, A. Nanayakkara, M. Challacombe, P. M. W. Gill, B. Johnson, W. Chen, M. W. Wong, J. L. Andres, C. Gonzalez, M. Head-Gordon, E. S. Replogle, and J. A. Pople, computer code GAUSSIAN98 Revision A.9 (Gaussian Inc., Pittsburgh, PA, 1998).
[67] G. Schaftenaar, computer code MOLDEN (The University of Nijmegen, Nijmegen, The Netherlands, 1991).
[68] (a) Y. Okamoto, computer code VLX (Fuji Photo Film Co., Ltd., Kanagawa, Japan, 2001); (b) Y. Yamakita, computer code LXVIEW (The University of Tokyo, Tokyo, Japan, 1995).
[69] R. Taylor and O. Kennard, J. Mol. Struct. **78**, 1 (1982).
[70] C. W. Bauschlicher, Jr. and H. Partridge, J. Chem. Phys. **103**, 1788 (1995).
[71] (a)K. Hoogsten, Acta Crystallogr. **12**, 822 (1959); (b) R. F. Stewart and L. H. Jensen, J. Chem. Phys. **40**, 2071 (1964).
[72] J. R. Ferraro, *Vibrational Spectroscopy at High External Pressures* (Academic Press Inc., New York, 1984), p. 2.
[73] (a) R. A. Crowell and E. L. Chronister, Chem. Phys. Lett. **195**, 602 (1992); (b) R. A. Crowell and E. L. Chronister, J. Phys. Chem. **96**, 9660 (1992). (c) B. J. Baer and E. L. Chronister, *ibid.* **99**, 7324 (1995).
[74] S. A. Hambir, J. Franken, D. E. Hare, E. L. Chronister, B. J. Baer, and D. D. Dlott, J. Appl. Phys. **81**, 2157 (1997).
[75] N. Liver, A. Nitzan, and J. I. Gersten, Chem. Phys. Lett. **111**, 449 (1984).